

Continual Learning of Multi-modal Dynamics with External Memory

Abdullah Akgül¹

Gozde Unal¹

Melih Kandemir²

¹Faculty of Computer and Informatics Engineering, Istanbul Technical University, Istanbul, Turkey

²Department of Mathematics and Computer Science, University of Southern Denmark, Odense, Denmark

Abstract

We study the problem of fitting a model to a dynamical environment when new modes of behavior emerge sequentially. The learning model is aware when a new mode appears, but it does not have access to the true modes of individual training sequences. We devise a novel continual learning method that maintains a descriptor of the mode of an encountered sequence in a neural episodic memory. We employ a Dirichlet Process prior on the attention weights of the memory to foster efficient storage of the mode descriptors. Our method performs continual learning by transferring knowledge across tasks by retrieving the descriptors of similar modes of past tasks to the mode of a current sequence and feeding this descriptor into its transition kernel as control input. We observe the continual learning performance of our method to compare favorably to the mainstream parameter transfer approach.

1 INTRODUCTION

Continual Learning (CL) aims to develop a versatile model that is capable of solving multiple prediction tasks which are presented to the model one task at a time. The model is then expected to learn the latest task as accurately as possible while preserving its excellence at the previous ones. Performance drop caused by the newly learned task is called *catastrophic forgetting*. Continual learning is essential for the development of intelligent agents that can adapt to new environmental conditions not encountered during training. For instance, an autonomous driving controller may improve its policy based on new experience collected during its customer-side life time. There exist a solid body of work that adopt parameter transfer across tasks as the key element of task memorization [Kirkpatrick et al., 2017, Nguyen

et al., 2018, Singh et al., 2019, Zenke et al., 2017]. There also appear preliminary studies on building attentive memories to capture tasks [Garnelo et al., 2018, Fraccaro et al., 2018]. However, established principles for building optimal memory mechanisms for continual learning are missing.

Probabilistic State-Space Models (SSM) are the standard framework for uncertainty-aware identification of complex dynamical systems. SSMs find widespread applicability to forecasting socio-economically impactful quantities such as weather, currency exchange, equity prices, and sales trends. SSM research gains significance also in robot learning parallel to the growing interest in model-based reinforcement learning [Deisenroth and Rasmussen, 2011, Hafner et al., 2019, 2020]. SSMs also set the fundamentals of stochastic optimal control [Åström, 2012], enhancing the impact potential of their thorough investigation even further.

We introduce a novel problem setup where dynamical system modeling tasks emerge sequentially and a probabilistic SSM is expected to learn them cumulatively. We further assume each task to follow multi-modal dynamics, where each individual sequences of a task follows one of the possible modes that describe the task. Successful continual learning in such a setup presupposes maximally efficient encoding of tasks into a long-term memory and their accurate retrieval. We curate a novel continual learning model tailored for addressing this very challenging problem. Our model captures the characteristics of unknown modes of sequences of the present task into fixed-sized vectors, called *mode descriptors*, stores these descriptors in an external neural episodic memory addressable via a learnable attention mechanism. Our model represents multiple task modes by feeding these mode descriptors into the state transition kernel as an additional input. We place a Dirichlet Process prior on the attention weights of the memory to encourage the explanation of the data with minimum number of modes. Figure 1 illustrates our model with external memory and the problem with two tasks and four modes. Our resulting Bayesian model can be efficiently trained using a straightforward adaptation of the established variational

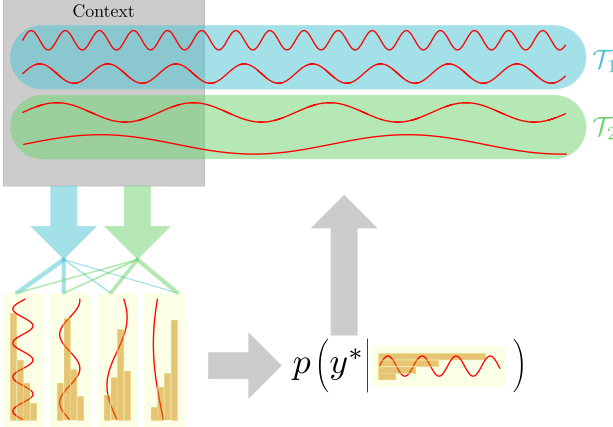


Figure 1: We study continual learning of dynamical systems, each operate on a non-overlapping set of multiple modes unknown to the learner at each task. We find out that inferring mode descriptors from an observed sequence snipped ($y_{1:C}$), storing them in an external neural episodic memory, retrieving them in the subsequent tasks, and feeding them into the state transition kernel as control input brings improved continual learning performance. We encourage efficient use of memory space by placing a Dirichlet Process (DP) prior on the effective count of encountered modes.

SSM inference techniques.

Studying continual learning in real dynamical systems requires continual environment intervention which is not feasible or many use cases. We instead create controlled flow of tasks generated from three challenging nonlinear multi-modal dynamical systems in order to control task similarities in a way eligible for continual learning. Our method exhibits consistent performance improvement over the established parameter transfer approach, verifying the importance of parsimonious use of neural episodic memory in efficient within-task knowledge acquisition and effective cross-tasks knowledge transfer.

2 PROBLEM SETUP: CONTINUAL MULTI-MODAL DYNAMICS LEARNING

We assume a learning agent that observes a dynamical environment via sequences $y_{1:T} = \{y_1, \dots, y_T\}$ consisting of time-indexed measurements $y_t \in \mathcal{Y}$ living in a measurable space \mathcal{Y} . We denote a snippet of a sequence $y_{t:t'} = \{y_t, \dots, y_{t'}\}$ for an arbitrary time interval $[t, t']$. We assume the dynamic environment to have some global characteristics with long-term impact, called its *mode*. We define the *mode* of a sequence $y_{1:T}$ as a fixed-sized vector $m \in \mathcal{X}$ defined in a K -dimensional embedding space that encodes the cumulative impact of the external factors on the

global properties of the environment dynamics of interest. We consider the realistic case that these global characteristics, which we refer to as *modes*. A dynamical system can potentially operate within a large number of modes. Making an analogy to the real world, an autonomous vehicle may need to account for a different environmental characteristics when planning and control for different weather conditions, countries, and times of a day. Only few of the modes are active for a particular time point and each mode instantly activates and deactivates for limited time periods.

We search for a learning algorithm that enable the agent to fit to a dynamical environment which has perpetually changing global characteristics. *We cast the corresponding learning problem as continual learning of multi-modal dynamical systems, where each task is defined as a group of modes that modulate a specific dynamical system.* In formal terms, a task \mathcal{T}_i is defined as a group of mode descriptors sampled from a mode generating oracle $P(\mathcal{X})$, that is

$$\mathcal{T}_i = \{m_r | m_r \sim P(\mathcal{X}), r = 1, \dots, R\}. \quad (1)$$

We assume each sequence within a task to be generated from dynamics modulated by a mode sampled from \mathcal{T}_i

$$\begin{aligned} \mathcal{D}_{\mathcal{T}_i} = \{y_{1:T}^n | m_n \sim P(\mathcal{T}_i), \\ y_{1:T}^n \sim p(y_{1:T} | m_n), n = 1, \dots, N\}, \end{aligned} \quad (2)$$

where $Pr(\mathcal{T}_i)$ is a probability mass function defined on the modes of task \mathcal{T}_i and $p(y_{1:T} | m_r)$ is the probability measure that describes the true behavior of the environment dynamics under mode m_r within a time interval $[1, T]$. The marginal distribution of a task with respect to its modes is given as

$$p(y_{1:T} | \mathcal{T}_i) = \sum_{r=1}^R p(y_{1:T} | m_r) P(m_r | \mathcal{T}_i). \quad (3)$$

The agent observes a task via a data set $\mathcal{D}_{\mathcal{T}_i}$ that contains only the sequences $y_{1:T}^n$ but not their corresponding modes.

We are interested in learning a model that minimizes the true continual learning risk functional below

$$\begin{aligned} R_{\mathbb{L}}^{CL}(h_{\theta}) = \lim_{U \rightarrow +\infty} \sum_{i=1}^U \mathbb{E}_{\mathcal{T}_i \sim P(\mathcal{X})} \bigg[\\ \mathbb{E}_{y_{1:T} \sim p(y_{1:T} | \mathcal{T}_i)} \big[\mathbb{L}(h_{\theta}(\cdot | y_{1:C}), y_{C+1:T}) \big] \bigg], \end{aligned} \quad (4)$$

which amounts to the limit of the cumulative risk of individual tasks as they appear one at a time. Above, $h_{\theta} : \mathcal{Y}^C \rightarrow \mathcal{Y}^{T-C}$ is a stochastic process that can map an observed sequence of an arbitrary length C to the subsequent $T - C$ time steps. We call the observations $y_{1:C}$ on the first C time steps h_{θ} conditions on as the *context* and define \mathbb{L} as a sequence-specific loss function defined on the future values of the sequence $y_{C+1:T}$. We evaluate the performance of predictions \hat{y} via two scores:

- **Normalized Mean Squared Error (NMSE):**

$$\mathbb{L}_{NMSE}(h_\theta(\cdot|y_{1:C}), y_{C+1:T}) = \mathbb{E}_{\hat{y}_{C+1:T} \sim h_\theta(\cdot|y_{1:C})} \left[\frac{\|\hat{y}_{C+1:T} - y_{C+1:T}\|_2^2}{\|y_{C+1:T}\|_2^2} \right] \quad (5)$$

as a measure of the prediction accuracy of h_θ when used as a Gibbs predictor, and

- **Negative Log-likelihood (NLL):**

$$\mathbb{L}_{NLL}(h_\theta(\cdot|y_{1:C}), y_{C+1:T}) = \log h_\theta(\hat{y}_{C+1:T}|y_{C+1:T}), \quad (6)$$

as a measure of Bayesian model fit that quantifies the model's own assessment on the uncertainty of its assumptions.

We approximate the true continual learning risk by its empirical counterpart

$$\hat{\mathbb{R}}_{\mathbb{L}}^{CL} = \frac{1}{N} \sum_{i=1}^U \sum_{n=1}^N \mathbb{L}(h_\theta(y_{C+1:T}^n|y_{1:C}^n) \mid \mathcal{T}_i) \quad (7)$$

for a finite number U of tasks presented to h_θ one at a time.

3 NOVEL BASELINE: VARIATIONAL CONTINUAL LEARNING FOR BAYESIAN STATE-SPACE MODELS

We build our target model on a Bayesian treatment of state-space modeling, which is proven to be effective in learning under high uncertainty and knowledge transfer across tasks, as practiced in the seminal prior art of continual learning [Kirkpatrick et al., 2017, Nguyen et al., 2018]. We perform approximate inference using variational Bayes due to its multiple successful applications to state-space models [Frigola et al., 2014, Doerr et al., 2018, Ialongo et al., 2019] and its favorable computational properties. As there does not exist any prior work tailored specifically towards continual learning for dynamical systems, we curate our own baseline. We adopt the established practice of setting the posterior of the learned parameters of the previous task as the prior of the next one. We choose the Variational Continual Learning (VCL) [Nguyen et al., 2018] approach, as it inherits all advantages of Elastic Weight Consolidation (EWC) [Kirkpatrick et al., 2017] but uses a more accurate posterior inference scheme.

Bayesian State Space Models (BSSM) are characterized by the data generating process below

$$\begin{aligned} \theta &\sim p(\theta), \\ x_0 &\sim p(x_0), \\ x_t|x_{t-1}, \theta &\sim p(x_t|x_{t-1}, \theta), \\ y_t|x_t &\sim p(y_t|x_t), \end{aligned} \quad (8)$$

where x_t and y_t correspond to the latent and observed state variables for time step t , respectively. The system dynamics are modeled by the first-order Markovian transition kernel $p(x_t|x_{t-1}, \theta)$ parameterized by θ that in turn follows a prior distribution $p(\theta)$. The latent states are mapped to the observation space via a probabilistic observation model $p(y_t|x_t)$. We formulate the initial latent state x_0 as another random variable that follows the prior distribution $p(x_0)$.

Variational Inference is required to approximate the posterior $p(x_{0:T}, \theta|y_{1:T})$, which will be intractable for many choices of distribution families for the data generating process in Eq. 8. Following [Yildiz et al., 2019], we choose the variational distribution to be mean-field across the parameters of the dynamics and the latent states

$$q_\psi(x_{0:T}, \theta|y_{1:T}) = q_\psi(x_0|y_{1:C}) \prod_{t=1}^T p(x_t|x_{t-1}, \theta) q(\theta). \quad (9)$$

This formulation has multiple advantages. Firstly, modeling the marginal posterior $q_\psi(x_0)$ on the initial latent state by amortizing on the context observations makes the Evidence Lower BOund (ELBO) calculation invariant to the context length. Secondly, adopting the prior transition kernel avoids duplicate learning of environment dynamics with twice as many free parameters and prevents training from instabilities caused by the inconsistencies between prior and posterior dynamics. Applying Jensen's inequality in the conventional way, the corresponding ELBO will be

$$\begin{aligned} &\log p(y_{1:T}) \\ &= \log \int_{X, \theta} p(y_{1:T}|x_{1:T}) p(x_{1:T}|\theta, x_0) p(x_0) p(\theta) \\ &= \log \int_{X, \theta} \left\{ \frac{p(y_{1:T}|x_{1:T}) p(x_{1:T}|\theta, x_0) p(x_0) p(\theta)}{p(x_{1:T}|\theta, x_0) q_\psi(x_0|y_{1:C}) q(\theta)} \right. \\ &\quad \left. \times q_\psi(x_0|y_{1:C}) p(x_{1:T}|\theta, x_0) q(\theta) \right\} \\ &\geq \mathbb{E}_{p(x_{1:T}|\theta, x_0) q_\psi(x_0|y_{1:C}) q(\theta)} [\log p(y_{1:T}|x_{1:T})] \\ &\quad - KL(q_\psi(x_0|y_{1:C}) || p(x_0)) - KL(q(\theta) || p(\theta)), \end{aligned} \quad (10)$$

where $KL(\cdot || \cdot)$ stands for the Kullback-Leibler (KL) divergence between the two distributions on its arguments, and $X = \{x_0, \dots, x_T\}$.

VCL for BSSMs can be implemented as follows. Having fitted the ELBO (\mathcal{L}) above on the data set for the first task which has observed sequences $\mathcal{D}_{\mathcal{T}_1}$, we attain $\psi_1^* = \max_\psi \mathcal{L}(\psi, \mathcal{D}_{\mathcal{T}_1})$. When the next task arrives with data $\mathcal{D}_{\mathcal{T}_2}$, we assign $p(\theta) \leftarrow q_{\psi_1^*}(\theta)$ and maximize the ELBO again $\psi_2^* = \max_\psi \mathcal{L}(\psi, \mathcal{D}_{\mathcal{T}_2})$. We repeat this process continually for every new coming task. We refer to this newly curated baseline in the rest of the paper as *VCL-BSSM*. We neglect the coresnet extension of VCL since its

application to BSSMs is tedious and its advantage is not demonstrated with sufficient significance in the static prediction tasks studied in the original work.

4 TARGET MODEL: THE CONTINUAL DYNAMIC DIRICHLET PROCESS

The commonplace Bayesian approach to continual learning transfers knowledge across tasks by assigning the learned posterior on the parameters of the previous task as the prior on the parameters of the current task. This is an effective approach when the subject of transfer is a feed-forward model, such as a classifier in supervised learning setup [Nguyen et al., 2018] or a policy network in reinforcement learning [Kirkpatrick et al., 2017]. *We conjecture that the existing parameter transfer Ansatz would not be sufficient for the transfer of more complex task properties such as modes of dynamical systems.* We address this problem by tailoring a novel continual learning approach from an original combination of an aged statistical machine learning tool, the Dirichlet process, with the newly emerging neural episodic memory and attention mechanisms.

Dirichlet Processes are stochastic processes defined on a countably infinite number of categorical outcomes, every finite subset of which follows a multinomial distribution drawn from a Dirichlet prior [Teh et al., 2006]. A Dirichlet Process (DP) is built on the Griffiths-Engen-McCloskey (GEM) distribution [Pitman et al., 2002]

$$\begin{aligned} \pi'_r | \alpha_0 &\sim \text{Beta}(1, \alpha_0), \\ \pi_r &= \pi'_r \prod_{j=1}^{r-1} (1 - \pi'_j), \\ \pi &= [\pi_1, \dots, \pi_R], \end{aligned} \quad (11)$$

which we denote in short hand as $\pi \sim \text{GEM}(\alpha_0, R)$. The GEM distribution can also be viewed a stick-breaking process [Sethuraman, 1994] where $\alpha_0 > 0$ is a scalar hyperparameter. The data generation process below is called a Dirichlet Process for a base measure $G_0(\mathcal{X})$ defined on a σ -algebra \mathbb{B} of \mathcal{X}

$$\begin{aligned} m_r &\sim G_0(\mathcal{X}), \\ \pi &\sim \text{GEM}(\alpha_0, R), \\ G | \pi &= \sum_{r=1}^R \pi_r \delta_{m_r}, \end{aligned} \quad (12)$$

where $\delta_x(A)$ is Dirac delta measure that takes value 1 if $x \in A$ and 0 otherwise for any measurable set $A \in \mathbb{B}$ and G is a categorical distribution with parameters π .

Neural Episodic Memory. We assume that the environment dynamics can be expressed within a measurable latent

embedding space $x_t \in \mathcal{X}$, and a sequence encoder $e_\lambda(x_{t:t'})$ for $t \leq t'$ that maps a sequence of latent embeddings into a fixed dimensional vector, as well as a neural memory $M = \{m_1, \dots, m_R\}$ consisting of R elements $m_r \in \mathcal{X}$ that live in the same space as latent embeddings x_t . We can construct a probability measure for \mathbb{B} from the memory M by updating

$$m_r \leftarrow (1 - w_r(y_{1:C}, m_r))m_r + w_r(y_{1:C}, m_r)e_\lambda(y_{1:C}) \quad (13)$$

for every single sequence to foster clustering where

$$w_r(y_{1:C}, m_r) = \frac{\exp(\langle m_r, e_\lambda(y_{1:C}) \rangle)}{\sum_{j=1}^R \exp(\langle m_j, e_\lambda(y_{1:C}) \rangle)} \quad (14)$$

for some similarity function $\langle \cdot, \cdot \rangle : \mathcal{X} \times \mathcal{X} \rightarrow \mathbb{R}^+$. Moreover, this construction imposes a memory attention mechanism, where the encoded mode descriptors attend to the memory elements. Here we make the fair assumption that the modality of a sequence can be identified also from the observation space, while we need to infer to the latent representations accurately to model the mode dynamics in detail. We choose an uninformative base measure that assigns equal prior probabilities to memory elements $G_0(M) = \sum_{k=1}^R \frac{1}{R} \delta_{m_r}$.

The full model. We complement the BSSM in Eq. 8 with an external neural episodic memory M that is updated for each observed sequence with the rule in Eq. 13. We place a DP prior on the retrieval of mode descriptors $m_r \in M$ to encourage the model to generate minimum number of modes. We also feed the retrieved mode descriptor into the transition kernel $p(x_t | x_{t-1}, m, \theta)$ as control input. The resultant model, which we call as the *Continual Dynamic Dirichlet Process (CDDP)*, follows the generative process

$$\begin{aligned} \pi &\sim \text{GEM}(\alpha_0, R), \\ m &\sim \sum_{k=1}^R \pi_r \delta_{m_r}, \\ \theta &\sim p(\theta), \\ x_0 &\sim p(x_0), \\ x_t | x_{t-1}, \pi, \theta &\sim p(x_t | x_{t-1}, m, \theta), \\ y_t | x_t &\sim p(y_t | x_t), \end{aligned} \quad (15)$$

where the memory capacity R is set to a bigger number than the total number of modes encountered during training.

Inference. Since $p(x_{0:T}, \theta | y_{1:T})$ is intractable, we approximate it by variational Bayes. We inherit the advantages of the inference scheme of the BSSM by choosing the variational distribution as

$$\begin{aligned} q_\psi(x_{0:T}, \theta, \pi | y_{1:T}) &= q_\psi(x_0 | y_{1:C}, \pi) \\ &\times \prod_{t=1}^T \prod_{r=1}^R p(x_t | x_{t-1}, m_r, \theta)^{\pi_r} q(\theta) q(\pi | y_{1:C}), \end{aligned} \quad (16)$$

where

$$\begin{aligned}
q(\theta) &= \mathcal{N}(\theta|\mu, \Sigma), \\
q(\pi|y_{1:C}) &= \text{Cat}(w_1(m_1, y_{1:C}), \dots, w_K(m_K, y_{1:C})), \\
q(x_0|y_{1:C}, \pi) &= \\
&\prod_{r=1}^R \mathcal{N}\left(x_t|v_1(m_r, e_\lambda(y_{1:C})), v_2(m_r, e_\lambda(y_{1:C}))\right)^{\pi_r}
\end{aligned} \tag{17}$$

with $x_0 \sim \mathcal{N}(0, I)$. In the expressions above, v_1 and v_2 refer to dense layers. The corresponding ELBO is then calculated following similar lines to Eq. 10

$$\begin{aligned}
&\log p(y_{1:T}) \tag{18} \\
&= \log \int_{X, \theta, \pi} p(y_{1:T}|x_{1:T})p(x_{1:T}|\theta, x_0, \pi)p(x_0)p(\theta)p(\pi) \\
&= \log \int_{X, \theta, \pi} \left\{ \frac{p(y_{1:T}|x_{1:T})p(x_{1:T}|\theta, x_0, \pi)p(x_0)p(\pi)p(\theta)}{p(x_{1:T}|\theta, x_0, \pi)q(x_0|y_{1:C})q(\pi|y_{1:C})q(\theta)} \right. \\
&\quad \left. \times p(x_{1:T}|\theta, x_0, \pi)q_\psi(x_0|y_{1:C})q(\pi|y_{1:C})q(\theta) \right\} \\
&\geq \mathbb{E}_{p(x_{1:T}|\theta, x_0, \pi)q(x_0|y_{1:C})q(\theta)q(\pi|y_{1:C})} [\log p(y_{1:T}|x_{1:T})] \\
&\quad - KL(q(x_0|y_{1:C})||p(x_0)) - KL(q(\theta)||p(\theta)) \\
&\quad - KL(q(\pi|y_{1:C})||p(\pi)).
\end{aligned}$$

where the additional KL term on the memory element retrieval probabilities is analytically tractable as

$$\begin{aligned}
&KL(q(\pi|y_{1:C})||p(\pi)) = \tag{19} \\
&\sum_{r=1}^R w_r(m_r, y_{1:C}) \log \left(\frac{w_r(m_r, y_{1:C})}{GEM(\alpha_0, R)_r} \right).
\end{aligned}$$

Prediction. Having trained the model on the latest task \mathcal{T}_i , its posterior predictive distribution for given new observation Y^* can be computed as

$$\begin{aligned}
p(Y_{C+1:T}^*|\mathcal{D}_{\mathcal{T}_i}, Y_{1:C}^*) &= \int_{X, \theta, \pi} q(x_0|Y_{1:C}^*)q(\theta) \times \tag{20} \\
&q(\pi|Y_{1:C}^*) \left[\prod_{t=C+1}^T p(y_t^*|x_t)p(x_t|x_{t-1}, \theta) \right].
\end{aligned}$$

Figure 2 summarizes the CDDP model design (top), and the corresponding training routine (bottom).

5 RELATED WORK

State Space Models. Deterministic SSMs, such as the Long Short-Term Memory (LSTM) [Hochreiter and Schmidhuber, 1997], the Gated Recurrent Unit (GRU) [Cho et al., 2014], and Transformer Nets [Vaswani et al., 2017] are in frequent use for sequential predictions. There exist a considerable body of work on Bayesian versions of SSMs that

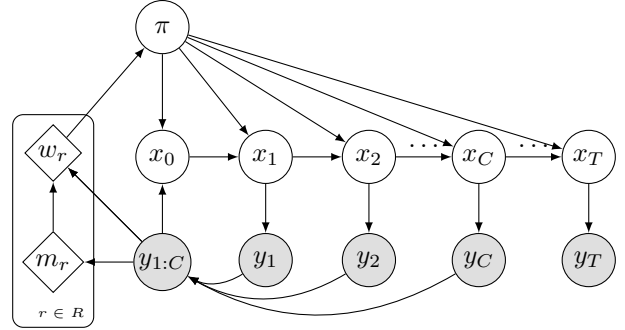


Figure 2: CDDP Plate Diagram (top). Shaded nodes are observed, unshaded nodes are latent and diamonds are deterministic. Arrows denote the conditional dependencies. The first C observations, called *the context*, amortize the inference of the initial hidden state, and also determine the content and addressing of the mode embeddings in the external memory. CDDP Training Routine (bottom).

employ Gaussian Process as transition kernels [Frigola et al., 2014, Doerr et al., 2018, Ialongo et al., 2019] and perform variational inference. SSMs introduce a stochastic variable called the latent for each time step. Another vein of work [Fraccaro et al., 2018, Hafner et al., 2019, 2020] model the transition dynamics as recurrent neural nets (RNN) that map a state to the next time step deterministically, while admitting a random state variable from the previous time step as input and feeding its output to the distribution of this variable at the subsequent time step.

Attention and Memory in Neural Nets. Neural Turing Machines (NTMs) [Graves et al., 2014] and Differential Neural Computers (DNC) [Graves et al., 2016] are first

examples of attention-based neural episodic memory use with external updates. Transformer Networks [Vaswani et al., 2017] introduce the notion of self attention and effectively use it in conjunction with cross attention to perform sequence-to-sequence prediction for long horizons. The Attentive Neural Process (ANP) [Kim et al., 2019] employs attention to build a neural stochastic process that is consistent over the observed predictions. It has been shown that an attention network can also be viewed as a Hopfield Network [Ramsauer et al., 2021], which explains its success at memorization of complex patterns. The Evidential Turing Process (ETP) [Kandemir et al., 2022] maintains an external memory that learns to feed a Dirichlet prior on the class distribution with informative concentration parameters inferred during minibatch training updates.

Continual Learning is a sub-problem of meta-learning [Finn et al., 2017, Snell et al., 2017] where new tasks are introduced one at a time and a base model is expected to learn the newest task without forgetting the previous ones. Unlike biological intelligence, artificial intelligence suffers from catastrophic forgetting in continual/lifelong learning. Early approaches to continual learning such as Synaptic intelligence (SI) [Zenke et al., 2017] and Elastic Weight Consolidation (EWC) [Kirkpatrick et al., 2017] transfer knowledge by the transfer of either deterministic parameters or their inferred distribution. SI calculates a plasticity measure by comparing the change rate of the gradients of the loss and the change rate of the synapses, whereas EWC uses Fisher information. Variational Continual Learning (VCL) [Nguyen et al., 2018] improves on EWC with a more comprehensive inference scheme and an additional feedback channel via a core set of most characteristic observations of past tasks. Generalized VCL (GVCL) [Loo et al., 2021] maximizes the same ELBO as VCL but using β -VAE to prevent the training instability caused by the dominance of the KL-divergence term. We do not use β -VAE since our setup does not have this problem. Sequential Neural Processes (SNP) [Singh et al., 2019] captures the evolution of parameters across tasks via a recurrent SSM that determines the sufficient statistics of a neural process prior. For the first time, our CDDP studies multi-modality in a continual learning setting. It is also the first model to transfer knowledge across tasks via learned mode descriptors that are maintained in an external memory.

6 EXPERIMENTS

We evaluate our CDDP by generating data from three challenging nonlinear dynamical systems. We prefer synthetic, yet challenging, prediction environments to maintain control on the level of similarity across tasks, which is essential for the interpretability of the numerical results of a continual learning setup. Too much task similarity would make continual learning unnecessary, while too much task difference

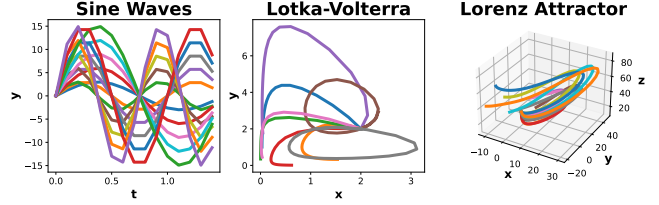


Figure 3: Sample sequences collected from different modes of the dynamical systems we consider for continual learning. Colors correspond to different modes. Sine Waves (*left*) has 15 modes of 1-D data, Lotka-Volterra (*middle*) has eight modes of 2-D data, and Lorenz Attractor (*right*) has 12 modes of 3-D data. For each data set, modes live in the same dynamical system but differ in the free parameters that govern the dynamics. For instance, the Sine Waves takes differ in magnitude and frequency.

would make it infeasible. When tasks share a reasonable degree of similarity, a successful continual learning algorithm is expected to capture, encode, and memorize these similarities and discard their differences. We generate modes that share similar dynamical properties, as their time evolution follows the same set of differential equations. However, modes differ from each other in the choice of the free parameters that govern the dynamical system. Figure 3 presents a sample visualization of modes that constitute the continual learning tasks on each of the three dynamical systems.

Sine Waves data set consists of signals grouped into modes described by different magnitudes and frequencies. Sine waves are created from the function $A \sin(2\pi f t)$ where A is the magnitude, f is the frequency and t is time. We generate different modes from five different choices for $A \in [3, 6, 9, 12, 15]$, and three frequency levels for $f \in [\frac{2}{3}, 1, \frac{4}{3}]$. We add Gaussian noise from $\mathcal{N}(0, \sigma)$ and set σ to $\frac{A}{100}$ for each mode to the train split.

Lotka-Volterra equations stem from modeling the dynamics of predator and prey populations. The Lotka-Volterra dynamics are defined by the first-order nonlinear differential equations: $dx_t/dt = \alpha x_t - \beta x_t y_t$, $dy_t/dt = \delta x_t y_t - \gamma y_t$. We generate different modes by setting the free parameter pairs (α, δ) and (β, γ) to different values. Starting with a fixed point $(x_0, y_0) = (2, 2)$, we select levels as $\alpha, \beta, \gamma \in [0.25, 0.75]$, and a constant $\delta = 0.5$. We add a Gaussian noise from $\mathcal{N}(0, 0.001)$ to the train split.

Lorenz Attractor is a three-dimensional nonlinear dynamical system developed originally to model atmospheric convection. As the Lorenz attractor is chaos-theoretic, hence not solvable with predictable consistency using the existing numerical methods, it is often used as a challenging environment to evaluate probabilistic dynamical models [Haußmann et al., 2021, Satorras et al., 2019]. The Lorenz

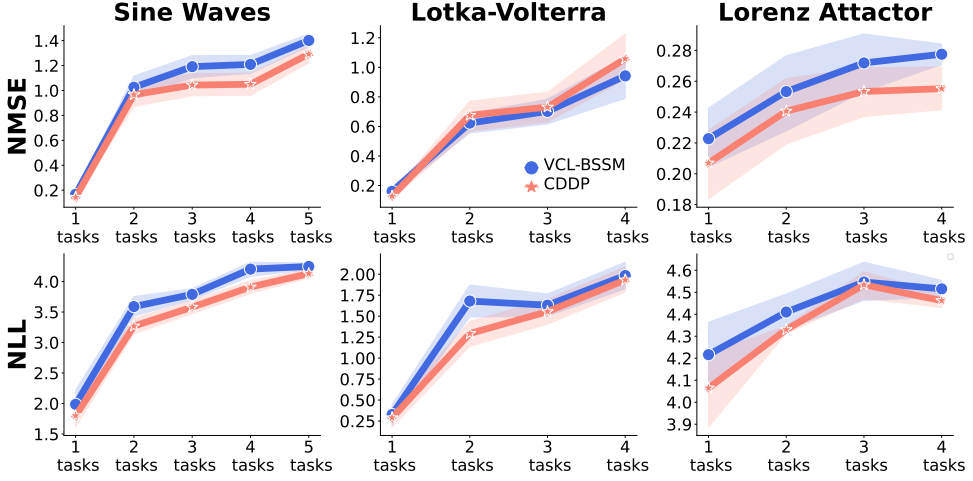


Figure 4: Our main results with means and standard errors of the scores across 20 repetitions for the Sine Waves and Lotka-Volterra and 10 repetitions for the larger Lorenz Attractor system. Our CDDP outperforms VCL in all three systems in terms of Negative Log-Likelihood (NLL) and in two of them in terms of Normalized Mean-Squared Error (NMSE).

system is described by $dx_t/dt = \sigma(y_t - x_t)$, $dy_t/dt = x_t(\rho - z_t) - y_t$, $dz_t/dt = x_t y_t - \beta z_t$. We determine our modes by setting the free parameters σ , ρ , and β of the Lorenz system to different values. We start with initial state $(x_0, y_0, z_0) = (1, 1, 28)$ and generate a long sequence. We generate modes with different but partially overlapping dynamical characteristics by setting ρ to three and σ and β to two different values. We select the three free parameters levels as $\rho \in [28, 42, 56]$, $\sigma \in [8, 12]$, and $\beta \in [\frac{5}{3}, \frac{13}{3}]$. We add Gaussian noise from $\mathcal{N}(0, 0.01)$ to the train split.

6.1 EXPERIMENTAL SETUP

We define each task as sequences coming from three modes. We use a different set of modes for each task without overlap. Each experiment repetition presents the tasks to the continual learning models at random order. We provide a PyTorch implementation of our full experiment pipeline that contain studied models as supplement to our submission, data generation process of all three dynamical systems, as well as the performance evaluation procedures. We will make the code base public upon acceptance.

Data. Each data set has 12 train sequences and 6 test sequences per mode. There are 15 modes 5 tasks in Sine Waves, 8 modes 4 tasks in Lotka-Volterra and 12 modes 4 tasks in Lorenz Attractor. We set the sequence lengths and time steps $(T, \Delta t)$ to $(15, 0.1)$ for Sine Waves, $(25, 0.4)$ for Lotka-Volterra, and $(50, 0.01)$ for the Lorenz Attractor. For each mode in the whole data set, we generate a long sequence and divide the whole sequence into subsequences of length T with a certain space between them. By adding additional Gaussian noise to the train split, we construct train and test splits with these subsequences.

Architectures. Our CDDP has four main architectural elements: i) Encoder: The sequence encoder $e_\lambda(x_{t:t'})$ governs the mean of our normal distributed recognition model $q_\psi(x_0|y_{1:C}, \pi)$. We choose the context size to be one-third of the sequence length for all three dynamical systems, amounting to five for Sine Waves, eight for Lotka-Volterra, and 16 for the Lorenz Attractor. We feed C observations as a stacked set of values into the encoder. The sequence encoder is a single dense layer for Sine Waves and Lotka-Volterra and a multi-layer perceptron for the Lorenz Attractor with two hidden layers of size 90. The perceptron uses the $\tanh(\cdot)$ activation function followed by layer normalization. ii) Decoder: The likelihood function $p(y_t|x_t)$ of the base model serves as a probabilistic decoder that maps the latent state x_t to the observed state y_t . We choose the emission distribution to be normal with mean governed by a single dense layer for Sine Waves and Lotka-Volterra and a multilayer perceptron with two hidden layers of size 90 for the Lorenz Attractor. The perceptron uses the $\tanh(\cdot)$ activation function followed by layer normalization. iii) Transition Kernel: We choose the transition kernel $p(x_t|x_{t-1}, m, \theta)$ of CDDP to be a normal distribution with mean governed by a plain RNN that receives a concatenation of the previous hidden state and the mode descriptor as input. All covariates are set to a fixed variance of 0.1. The RNN on the mean is a multilayer perceptron with one hidden layer of size 40 for Sine Waves and Lotka-Volterra and 90 for the Lorenz Attractor. The perceptron uses the $\tanh(\cdot)$ activation function followed by layer normalization. The transition kernel of the base model of VCL $p(x_t|x_{t-1}, \theta)$ follows the same RNN architecture except that its input does not contain a mode descriptor. iv) External Memory: We set the memory size to 20 for the Sine Wave environment, 10 for Lotka-Volterra, and 15 for the Lorenz Attractor.

Table 1: Ablation study results on the Sine Waves data set as mean \pm standard errors over all tasks across five repetitions.

	Parameter Transfer	Probabilistic Parameters	Memory Content	NMSE	NLL
RNN	✓	✗	N/A	1.035 ± 0.132	3.498 ± 0.280
VCL-BSSM	✓	✓	N/A	0.931 ± 0.104	3.560 ± 0.227
CDDP Variants	✗	✓	Zeros	0.944 ± 0.105	3.565 ± 0.232
	✗	✓	Ones	1.118 ± 0.114	3.749 ± 0.197
	✗	✓	Twos	1.351 ± 0.148	3.795 ± 0.180
	✓	✓	Learned	0.906 ± 0.105	3.900 ± 0.210
CDDP Target	✗	✓	Learned	0.865 ± 0.100	3.346 ± 0.213

6.2 RESULTS AND ABLATION STUDY

Main Results. Figure 4 depicts our main results for the evolution of model performance as the number of tasks grows. Our CDDP outperforms the parameter transfer based VCL-BSSM baseline consistently in all three dynamical systems with respect to *NLL* and two of them respect to *NMSE*, while being on par on the third. Storing mode descriptors of the learned dynamics in an external memory, retrieving them in the subsequent tasks and feeding them into the state transition kernel prevents catastrophic forgetting more effectively than plain parameter transfer. The details of the numerical results are provided in Appendix, Table 2.

Computational Cost. The difference of the computational footprints of our neural episodic memory based approach and the parameter transfer approach is negligible. The average wall-clock Time Per Epoch (TPE) measured on the Sine Wave data set for VCL-BSSM is 0.200 ± 0.002 and 0.208 ± 0.002 seconds for our CDDP. We expect the computational cost of CDDP to increase linearly with respect to memory size, which is balanced by its parsimonious use of memory content by virtue of the Dirichlet Process prior.

Ablation Study. We investigate the contribution of individual design choices into the total performance of our target model. We study the effect of three design choices: i) knowledge transfer via parameters θ of the learned transition dynamics, ii) quantifying the uncertainty of the parameters of transition dynamics by a distribution $q(\theta)$, and iii) maintaining an external memory with learned or unlearned content. Table 1 shows a map of model variants corresponding to the activation status of these three design choices, as well as the corresponding numerical results on the Sine Waves data set over five repetitions. We observe the higher performance to come when knowledge transfer is done via the external memory *instead of* —*but not together with* — parameter transfer, supporting the central assumptions of our target model. Setting the memory content to unlearned values causes rapid performance deterioration as values diverge from the learned values. This outcome provides additional evidence for the essential role the external memory plays in the continual learning performance of CDDP.

7 CONCLUSION

Summary. We report the first study on continual learning of multi-modal dynamical systems. We curate a competitive baseline for this new problem setup from an adaptation of VCL to BSSMs. We introduce a novel alternative to the parameter transfer approach of VCL for within-task knowledge acquisition and cross-tasks knowledge transfer using an original combination of neural episodic memory, Dirichlet processes, and BSSMs. We observe in continual learning of three challenging dynamics modeling environments that our alternative approach compares favorably to the established parameter transfer approach.

Broad Impact. Our work can be used in numerous areas of applied research such as weather forecasting, where features can be transferred from one climate to another, autonomous driving, where data can be adapted across different countries drivers, model-based reinforcement learning algorithms when the environment changes due either to the actions of the ego agent or to external factors. The memory architecture of CDDP may be improved by alternative embedding, update, and attention mechanisms. The plain RNN that governs the transition kernel of the base model may be replaced by Transformer Networks [Vaswani et al., 2017], Neural Stochastic Differential Equations [Hausmann et al., 2021], or a blend of recent approaches.

Limitations and Ethical Concerns. CDDP demonstrates high sensitivity to the performance of its base model on individual tasks. The interpretability of the memory descriptors of the CDDP deserves further investigation. The generalizability of our results to real-world dynamics data could be a topic of a separate study. We present CDDP as a general-purpose method, hence its use in fairness-sensitive applications may require post-hoc allocation of existing fairness-inducing algorithms. The uncertainty calibration footprint of CDDP calls for another empirical study prior to its deployment into a safety-critical setup.

References

K.J. Åström. *Introduction to stochastic control theory*. Courier Corporation, 2012.

K. Cho, B. van Merriënboer, D. Bahdanau, and Y. Bengio. On the properties of neural machine translation: Encoder-decoder approaches. *arXiv preprint arXiv:1409.1259*, 2014.

M.P. Deisenroth and C. Rasmussen. PILCO: A model-based and data-efficient approach to policy search. In *ICML*, 2011.

A. Doerr, C. Daniel, M. Schiegg, N. Duy, S. Schaal, M. Tous-saint, and T. Sebastian. Probabilistic recurrent state-space models. In *ICML*, 2018.

C. Finn, P. Abbeel, and S. Levine. Model-agnostic meta-learning for fast adaptation of deep networks. In *ICML*, 2017.

M. Fraccaro, D.J. Rezende, Z. Zwols, A. Pritzel, S.M.A. Eslami, and F. Viola. Generative temporal models with spatial memory for partially observed environments. In *ICML*, 2018.

R. Frigola, Y. Chen, and C. E. Rasmussen. Variational Gaussian process state-space models. In *NeurIPS*, 2014.

M. Garnelo, J. Schwarz, D. Rosenbaum, F. Viola, D.J. Rezende, S.M. Eslami, and Y.W. Teh. Neural processes. *arXiv preprint arXiv:1807.01622*, 2018.

A. Graves, G. Wayne, and I. Danihelka. Neural Turing Machines. *arXiv preprint arXiv:1410.5401*, 2014.

G. Graves, G. Wayne, M. Reynolds, T. Harley, I. Danihelka, A. Grabska-Barwinska, S.G. Colmenarejo, E. Grefenstette, T. Ramalho, J. Agapiou, A.P. Badia, K.M. Hermann, Y. Zwols, G. Ostrovski, A. Cain, H. King, C. Summerfield, P. Blunsom, K. Kavukcuoglu, and D. Hassabis. Hybrid computing using a neural network with dynamic external memory. *Nature*, 538:471–476, 2016.

D. Hafner, T. Lillicrap, I. Fischer, R. Villegas, D. Ha, H. Lee, and J. Davidson. Learning latent dynamics for planning from pixels. In *ICML*, 2019.

D. Hafner, T. Lillicrap, J. Ba, and M. Norouzi. Dream to control: Learning behaviors by latent imagination. In *ICLR*, 2020.

M. Haußmann, S. Gerwinn, A. Look, B. Rakitsch, and M. Kandemir. Learning partially known stochastic dynamics with empirical PAC Bayes. In *AISTATS*, 2021.

S. Hochreiter and J. Schmidhuber. Long short-term memory. *Neural computation*, 9:1735–80, 12 1997.

A.D. Ialongo, M. van der Wilk, J. Hensman, and C.E. Rasmussen. Overcoming mean-field approximations in recurrent Gaussian process models. In *ICML*, 2019.

M. Kandemir, A. Akgül, M. Haussmann, and G. Unal. Evidential Turing processes. In *ICLR*, 2022.

H. Kim, A. Mnih, J. Schwarz, M. Garnelo, A. Eslami, D. Rosenbaum, O. Vinyals, and Y.W. Teh. Attentive neural processes. In *ICLR*, 2019.

D.P. Kingma and J. Ba. Adam: A method for stochastic optimization. *arXiv preprint arXiv:1412.6980*, 2014.

J. Kirkpatrick, R. Pascanu, N. Rabinowitz, J. Veness, G. Desjardins, A.A. Rusu, K. Milan, J. Quan, T. Ramalho, A. Grabska-Barwinska, D. Hassabis, C. Clopath, D. Kumaran, and R. Hadsell. Overcoming catastrophic forgetting in neural networks. *Proceedings of the National Academy of Sciences*, 114(13), 2017.

N. Loo, S. Swaroop, and R.E. Turner. Generalized variational continual learning. In *ICLR*, 2021.

C.V. Nguyen, Y. Li, T.D. Bui, and R.E. Turner. Variational continual learning. In *ICLR*, 2018.

J. Pitman et al. Combinatorial stochastic processes. Technical report, 2002.

H. Ramsauer, B. Schäfl, J. Lehner, P. Seidl, M. Widrich, T. Adler, L. Gruber, M. Holzleitner, M. Pavlovic', G.K. Sandve, V. Greiff, D. Kreil, M. Kopp, G. Klambauer, J. Brandstetter, and S. Hochreiter. Hopfield networks is all you need. In *ICLR*, 2021.

V.G. Satorras, Z. Akata, and M. Welling. Combining generative and discriminative models for hybrid inference. In *NeurIPS*, 2019.

J. Sethuraman. A constructive definition of Dirichlet priors. *Statistica Sinica*, 4(2):639–650, 1994.

G. Singh, J. Yoon, Y. Son, and S. Ahn. Sequential neural processes. In *NeurIPS*, 2019.

J. Snell, K. Swersky, and R.S. Zemel. Prototypical networks for few-shot learning. In *NeurIPS*, 2017.

Y.W. Teh, M.I. Jordan, M.J. Beal, and D.M. Blei. Hierarchical Dirichlet processes. *Journal of the American Statistical Association*, 101(476):1566–1581, 2006.

A. Vaswani, N. Shazeer, N. Parmar, J. Uszkoreit, L. Jones, A.N. Gomez, L. Kaiser, and I. Polosukhin. Attention is All you Need. In *NeurIPS*, 2017.

C. Yıldız, M. Heinonen, and H. Lähdesmäki. ODE²VAE: Deep generative second order ODEs with Bayesian neural networks. In *ICML*, 2019.

F. Zenke, B. Poole, and S. Ganguli. Continual learning through synaptic intelligence. In *ICML*, 2017.

APPENDIX

A EXPERIMENTAL DETAILS

We select Adam [Kingma and Ba, 2014] as optimizer with learning rates of 0.005 for Sine Waves, 0.001 for Lotka-Volterra, and 0.0005 for Lorenz Attractor. For all data sets, the batch size is equal to 9. We train the models 300 for Sine Waves, 750 for Lotka-Volterra, and 500 for Lorenz Attractor epochs per task .

B DETAILED MAIN RESULTS

Table 2: Quantitative results of models on three nonlinear dynamics. The table below reports mean \pm standard error across multiple repetitions.

		1 Task		2 Tasks		3 Tasks		4 Tasks		5 Tasks	
		NMSE	NLL								
Sine Waves	VCL-BSSM	0.167 \pm 0.024	1.986 \pm 0.240	1.026 \pm 0.096	3.589 \pm 0.160	1.191 \pm 0.090	3.790 \pm 0.097	1.209 \pm 0.075	4.204 \pm 0.120	1.402 \pm 0.057	4.247 \pm 0.057
	CDDP	0.143 \pm 0.014	1.799 \pm 0.191	0.966 \pm 0.090	3.270 \pm 0.134	1.044 \pm 0.094	3.579 \pm 0.116	1.050 \pm 0.090	3.910 \pm 0.103	1.292 \pm 0.071	4.130 \pm 0.081
Lotka-Volterra	VCL-BSSM	0.160 \pm 0.020	0.327 \pm 0.122	0.623 \pm 0.069	1.680 \pm 0.198	0.702 \pm 0.089	1.631 \pm 0.136	0.942 \pm 0.146	1.984 \pm 0.168		
	CDDP	0.128 \pm 0.019	0.289 \pm 0.121	0.675 \pm 0.109	1.293 \pm 0.153	0.731 \pm 0.103	1.554 \pm 0.158	1.054 \pm 0.158	1.932 \pm 0.156		
Lorenz Attractor	VCL-BSSM	0.223 \pm 0.020	4.216 \pm 0.157	0.253 \pm 0.026	4.410 \pm 0.085	0.272 \pm 0.021	4.547 \pm 0.094	0.278 \pm 0.007	4.515 \pm 0.041		
	CDDP	0.207 \pm 0.023	4.065 \pm 0.189	0.241 \pm 0.024	4.330 \pm 0.019	0.253 \pm 0.018	4.534 \pm 0.062	0.255 \pm 0.015	4.462 \pm 0.033		